This is a preprint, the final version is subject to change, of the American Mineralogist (MSA)
Cite as Authors (Year) Title. American Mineralogist, in press.
(DOI will not work until issue is live.) DOI: http://dx.doi.org/10.2138/am.2013.4358

Fe-rich and As-bearing vesuvianite and wiluite from Kozlov, Czech Republic

LEE A. GROAT,[1,*] R. JAMES EVANS,[1] JAN CEMPÍREK,[1] CATHERINE McCAMMON[2], AND STANISLAV HOUZAR[3]

[1]Department of Earth, Ocean and Atmospheric Sciences, University of British Columbia, Vancouver, British Columbia V6T 1Z4, Canada

[2]Bayerisches Geoinstitut, Universität Bayreuth, D-95440 Bayreuth, Germany

[3]Department of Mineralogy and Petrography, Moravian Museum, Zelný trh 6, 659 37 Brno, Czech Republic

*E-mail: groat@mail.ubc.ca

ABSTRACT

Green vesuvianite crystals occur with garnet and calcite in a hand specimen from the Nedvědice marble near Kozlov (near Štěpánov nad Svratkou, Svratka Crystalline Complex) in the Czech Republic. The average electron microprobe composition of the vesuvianite shows 12.10 wt.% Fe_2O_3 (4.66 Fe pfu), 2.77 wt.% B_2O_3 (2.45 B pfu), 1.71 wt.% As_2O_5 (0.46 As pfu), and 1.40 wt.% F (2.26 F pfu). The Fe concentration is the highest ever recorded for a vesuvianite-group mineral. The boron contents are extremely variable and two of the five compositions show more than the 2.50 B pfu needed for wiluite, and the average is only slightly less than this. The crystal structure [a = 15.7250(4), c = 11.7736(3) Å] was refined in space group $P4/nnc$ to an R_1 value of 0.0221. The site refinement and Mössbauer spectroscopy results show Fe^{2+} substituting for Ca at the X3 site and filling the Y1 position, and Fe^{3+} substituting for Al at the Y3 position. Most of the Fe (70% from the site refinements and 78% from the Mössbauer interpretation) is ferric. The main effect of the high Fe concentration is to increase the mean Y3–O distance to an unusually large 2.018 Å. Boron occurs at the T1 site, where it is coordinated by oxygen atoms at two O7B and two O11 positions, and at the T2 sites where it is coordinated by O atoms at one O10 and two O12A sites. When the nearby X3 site contains Fe, the T2 position is either vacant or [3]-coordinated by some combination involving an O10 site and two O12B positions, in which case the B atom is likely offset from the T2 site to reduce the B-O12B distance.

Fluorine and OH occupy the O11 positions when there is a vacancy at the adjacent T1 position. Pentavalent As substitutes for Si at the Z2 site and Al at the Y2 site. The $P4/nnc$ symmetry indicates that this vesuvianite formed at high temperatures (400-800 ºC) and the predominance of Fe^{3+} and As^{5+} suggests under oxidizing conditions.

The results showing Fe at three different sites with three different coordinations attests to the flexibility of the vesuvianite crystal structure. The incorporation of As at two different sites in the structure shows that rock-forming silicate minerals such as vesuvianite can be a reservoir for this heavy element.

Keywords: Vesuvianite, wiluite, iron, Czech Republic, arsenic, crystal structure.

INTRODUCTION

Vesuvianite is a rock-forming or accessory silicate mineral found in metamorphic rocks, rodingites, and altered alkaline rocks. From a crystal chemical point of view the formula of vesuvianite may be written as $X_{19}Y_{13}Z_{18}O_{69}(OH,F)_9$, where X are seven- to ninefold-coordinated, Y has octahedral or square pyramidal coordination, and Z represents tetrahedral coordination. The X positions are commonly occupied by Ca, the Y sites by Al, Mg, and Fe, and the Z positions by Si. The vesuvianite structure (Fig. 1) is closely related to that of grossular, but differs from it by having additional X4 and Y1 sites (site nomenclature from Groat et al. 1992a), the latter with square pyramidal coordination, at various levels along the fourfold axes. It is assumed that the X4 and Y1 periodicity is preserved within a single channel, but adjacent channels may have X4 and Y1 at different *z* levels (e.g., Giuseppetti and Mazzi 1983; Fitzgerald et al. 1986; Allen and Burnham 1992; Pavese et al. 1998; Armbruster and Gnos 2000a, b). The different X4 and Y1 arrangements lead to various tetragonal space goups. Allen and Burnham (1992) showed that ordered channel arrangements are favoured in vesuvianites grown at <300 ºC, and such crystals exhibit either *P*4/*n* or *P*4*nc* symmetry. In addition, a crystal might be assembled of domains representing both space groups, in which case the resulting space group becomes *P*4. Vesuvianites grown at 400-800 ºC exhibit disordered channel arrangements and the resulting symmetry is *P*4/*nnc* (Allen and Burnham 1992). Galuskin et al. (2003) suggested that the degree of order is also influenced by substitutions at the channel sites.

Groat et al. (1994, 1996) reported that some vesuvianite samples contain B at the T1 (0.055, 0.055, ¼) and T2 (¼, ¼, ¼) sites and Groat et al. (1998) described the new vesuvianite-group mineral wiluite defined as having more than 2.5 B atoms per formula unit (apfu). Groat et al. (1992b) showed that F substitutes for OH at both the O10 and O11 sites in the vesuvianite structure and Britvin et al. (2003) described the new vesuvianite-group mineral fluorvesuvianite defined as containing more than 4.5 F apfu.

Hrazdil et al. (2009, 2011) described a rare but geochemically significant calc-silicate skarn discovered in Nedvědice marble near Kozlov (near Štěpánov nad Svratkou, Svratka Crystalline Complex) in the Czech Republic. The rock was reported to contain a distinctive Sn-, As- rich mineral assemblage comprising largely green Sn-bearing (1.2–2.4 wt.% SnO_2) andradite with sporadic grossularite relics, As-bearing (≤1.97 wt.% As_2O_5) vesuvianite, malayaite and

accessory As-bearing fluorapatite, nordenskiöldine, and cassiterite. Hrazdil et al. (2009) identified two main stages of development of the mineral assemblage. The first, relatively high-temperature stage produced early grossularite, diopside and clinozoisite, and late Sn-bearing andradite, malayaite, and As-bearing vesuvianite. In the second retrograde alteration stage stokesite, "hydrocassiterite" and unidentified Ca-Fe-arsenates replaced minerals of the first stage. Hrazdil et al. (2009) suggested that the primary Fe-poor and Fe-rich assemblages crystallized under oxidizing conditions with highly variable Si activity and CO_2 fugacity and Fe-rich fluids enriched in B, As and Sn, at temperatures above 300 ºC.

Inspection of the compositions in Hrazdil et al. (2009) reveal that their vesuvianite samples are very high in Fe, with an average of 11.18 wt.% Fe_2O_3 (4.21 Fe pfu). This is much higher than the 8.10 and 7.59 wt.% FeO (3.44 and 3.21 Fe^{2+} pfu) reported by Fitzgerald et al. (1992) for vesuvianite samples from Pajsberg, Sweden; the 7.93 and 7.55 wt.% FeO (3.54 and 3.81 Fe^{2+} pfu) listed by Eby et al. (1993) for a partly metamict vesuvianite sample from the Seward Peninsula in Alaska; the 7.89 wt.% Fe_2O_3 reported by Bellatriccia et al. (2005a) for a wiluite from Ariccia in Italy; or the 7.51 wt.% FeO + Fe_2O_3 (1.59 Fe^{2+} and 1.46 Fe^{3+} pfu) described by Groat et al. (1996) for a wiluite from the Bill Waley mine in Tulare County, California.

Arsenic is rare in vesuvianite but Pan and Fleet (1992) reported up to 0.59 wt.% As_2O_5 (0.17 As pfu) in antimonian (up to 21.21 wt.% Sb_2O_3, or 4.88 Sb pfu) vesuvianite from the Hemlo gold deposit in Ontario. The As was assumed to replace Si at the Z sites. Groat and Evans (2012) reported up to 0.62 wt.% As_2O_5 (0.16 As^{5+} pfu) in Bi- and Mn-bearing vesuvianite from Långban, Sweden. They showed that the As occupies the T1 site and is coordinated by oxygen atoms at two O7B and two O11 positions.

We undertook this study to investigate the incorporation of Fe and As into the crystal structure of vesuvianite from this locality.

EXPERIMENTAL

Examination of the hand sample described by Hrazdil et al. (2009) revealed layers of green garnet and vesuvianite (indistinguishable to the naked eye) and white calcite alternating with layers of grey calcite. X-ray powder diffraction data confirmed the presence of vesuvianite, garnet and calcite.

A polished thin section was created from this sample. Investigation with a petrographic microscope showed that the vesuvianite is a pale green color in plane-polarized light and examination of grain mounts (using a refractive index oil with $n = 1.720$) showed that the mineral is uniaxial positive.

Several crystals were subsequently removed from the polished thin section with a microscope-mounted drill (manufactured by U. Medenbach, Witten, Germany) and were attached to glass fibers with epoxy for single-crystal X-ray diffraction study.

After collection of X-ray diffraction data, the crystal with the highest refined Fe content was attached to a Lucite disk with Petropoxy and polished for the electron microprobe study.

Powder X-ray-diffraction experiments were done with a Siemens D5000 diffractometer equipped with a diffracted-beam graphite monochromator, incident beam Soller slit, 2 mm divergence and antiscatter slits, and a 0.6 mm receiving slit. The normal-focus Cu X-ray tube was operated at 40 kV and 30 mA. Powder-diffraction data were collected over ranges of 10 to 70º 2θ, using scanning steps of 0.02º 2θ. Peak positions plus internal standard mixture were measured by Rietveld refinement using the program DBWS-9807 (Young et al. 1995). Cu$K\alpha_1$ peaks were corrected for cell refinement by reference to the internal standard (NIST Si 640c). Unit-cell dimensions were determined from the corrected X-ray powder-diffraction data using the program UnitCell (Holland and Redfern 1997).

The sample was also examined with a Philips XL30 scanning electron microscope (SEM) at the University of British Columbia, which is equipped with an energy-dispersion X-ray spectrometer (EDS).

Single-crystal X-ray diffraction measurements were made at C-HORSE (the Centre for Higher Order Structure Elucidation, in the Department of Chemistry at UBC) using a Bruker X8 APEX II diffractometer with graphite monochromated Mo$K\alpha$ radiation. The data were collected at room temperature to a maximum 2θ value of 66.3°. Data were collected in a series of φ and ω scans in 0.50° oscillations with 10.0 second exposures. The crystal-to-detector distance was 40 mm. Data were collected and integrated using the Bruker SAINT software package (Bruker 2007). Data were corrected for absorption effects using the multi-scan technique (SADABS, Sheldrick 1996) and were corrected for Lorentz and polarization effects.

All refinements were performed using the SHELXTL crystallographic software package (Sheldrick 2008) of Bruker AXS. Scattering factors for neutral atoms were used for the cations

and ionic factors for O^{2-} from Azavant and Lichanot (1993) were used for oxygen. The weighting scheme was based on counting statistics. Neutral atom scattering factors were taken from Cromer and Waber (1974). Anomalous dispersion effects were included in F_{calc} (Ibers and Hamilton 1964); the values for $\Delta f'$ and $\Delta f''$ were those of Creagh and McAuley (1992). The values for the mass attenuation coefficients are those of Creagh and Hubbell (1992).

The crystal structures were initially refined in space group *P*4/*nnc* using parameters (including T1, T2, O12, and split O7 sites) from the boron-bearing vesuvianite of Groat et al. (1996) and the site nomeclature of Groat et al. (1992a). The crystal structure reported here refined to an R_1 index of 0.0549 for an anisotropic displacement model with fixed site-scattering values for all atoms except those at T1, T2, and O12.

At this stage the site-scattering values for the cations were allowed to vary freely. The results suggested limited substitution of a heavier cation at the X3, Y2, Y3, and Z2 positions. Accordingly, Fe was refined against Ca at the X3 site and against Al at the Y3 position, and As was refined against Al at the Y2 site and against Si at the Z2 position. At this point the atom at the O12 site had very large displacement parameters which were modeled by splitting the site into two positions. The final R_1 value was 0.0221.

In order to examine structure details and visualize observed electron densities, the measured data were also refined using Jana2006 (Petricek et al. 2006) and electron density was visualized in 3D using VESTA 3 (Momma and Izumi 2011).

According to Armbruster and Gnos (2000a), speculation that many vesuvianites refined in space group *P*4/*nnc* are actually long-range ordered *P*4*nc* can be ruled out because the refinement results in a high R_1 value. In addition, they noted that if the structure of a long-range ordered vesuvianite of true space group *P*4*nc* is erroneously refined in space group *P*4/*nnc*, then F_o^2 is always greater than F_c^2 in the list of most disagreable reflections. This effect is especially pronounced for weak reflections, such as 147, 013, 057, 143 and 077. No such distribution was seen in the lists for our vesuvianite data.

Armbruster and Gnos (2000a) also describe another test where $F_c/F_c(\max)$ values are divided into 10 groups based on magnitude and a *K* value [where $K = \text{mean}(F_o^2)/\text{mean}(F_c^2)$] is determined for each group. An incorrect model or space group increases the *K* values of the weakest vesuvianite reflections up to a value of 10. The highest *K* value for this refinement was 1.007.

Electron microprobe compositions were obtained with a fully-automated CAMECA SX-100 microprobe at the Laboratory of Electron Microscopy and Microanalysis in Brno (a joint facility of Masaryk University and the Czech Geological Survey). The instrument was operated in the wavelength-dispersion mode with the following operating conditions: excitation voltage, 15 kV (B 5 kV); beam current, 10 nA (B 100 nA); peak count time, 20 s; background count time, 10 s; spot diameter, 20 μm. Data reduction was done using the "PAP" $\phi(\rho Z)$ method (Pouchou and Pichoir 1985). For the elements considered, the following standards, X-ray lines and crystals were used: datolite, B*K*α, PC2; topaz, F*K*α, PC1; $MgAl_2O_4$, Mg*K*α, LIF; sanidine, Al*K*α, TAP; titanite, Si*K*α, TAP; grossular, Ca*K*α, PET; spessartine, Mn*K*α, LIF; andradite, Fe*K*α, LIF; gahnite, Zn*K*α, LIF; lammerite, As*L*α, TAP; and Sn, Sn*L*α, PET. Formulae were calculated from the electron microprobe data on the basis of 50 cations (less B), which assumes no vacancies at the cation sites and only B at the T positions.

For the Mössbauer study the sample powder (72 mg) was mounted in a plastic sample holder with 12 mm diameter, resulting in an effective thickness of roughly 5 mg Fe/cm^2. A Mössbauer spectrum was recorded at room temperature (293 K) in transmission mode on a constant acceleration Mössbauer spectrometer with a nominal 1.85 GBq ^{57}Co source in a 6 micron Rh matrix. The velocity scale was calibrated relative to 25 μm thick α-Fe foil using the positions certified for (former) National Bureau of Standards standard reference material no. 1541; line widths of 0.28 mm/s for the outer lines of α-Fe were obtained at room temperature. The spectrum was collected for 3 days and fit to Lorentzian lines using the program MossA (Prescher et al. 2012).

Raman spectra were obtained with a Raman microscope system (InVia, Renishaw, Gloucestershire, U.K.) equipped with 785 nm excitation laser. Raman spectra were collected in the spectral range from 500 to 2000 cm^{-1} using a 50 × objective lens, 20 s exposure times, and ~7 mW excitation power.

RESULTS

Compositions

Electron microprobe compositions of the crystal used for the single-crystal X-ray diffraction study are reported in Table 1. The average composition shows 1.71 wt.% As_2O_5 (0.46 As pfu) and 12.10 wt.% Fe_2O_3 (4.66 Fe pfu), similar to the values reported by Hrazdil et al. (2009). As far as we are aware this is the highest Fe concentration ever reported for a vesuvianite-group mineral. The average composition also shows a moderate amount of F (1.40 wt.% F, 2.26 F pfu) which when plotted on the graph of Fe^{2+}/Fe^{3+} versus F from Groat et al. (1992a), suggests that most of the Fe is trivalent.

The boron contents are extremely variable and range from 2.25 to 3.40 wt.% B_2O_3 (2.00 to 2.97 B pfu). Two of the five compositions show more than the 2.50 B pfu needed for wiluite as defined by Groat et al. (1998), and the average content of 2.46 B pfu is only slightly less than this.

The Al content (average of 8.81 wt.% Al_2O_3, 5.31 Al pfu) is very low; the only compositions we are aware of with less Al are from the REE-bearing and Ti-rich vesuvianite from San Benito County, California with 5.54 (3.60 Al pfu; Groat et al. 1992a) and 4.35 wt.% Al_2O_3 (Fitzgerald et al. 1987). The average Mg content of the structure crystal is 4.40 wt.% MgO (3.36 Mg pfu).

The compositions show less Ca (average 33.66 wt.% CaO, 18.45 Ca pfu) and Si (34.49 wt.% SiO_2, 17.65 Si pfu) than needed to fill the X and Z sites, respectively, which suggests substitutions or vacancies at those positions.

The compositions also show minor amounts of Mn (average 0.13 wt.% MnO, 0.06 Mn pfu), Zn (average 0.11 wt.% ZnO, 0.04 Zn pfu), and Sn (average 0.09 wt.% SnO_2, 0.02 Sn pfu).

Unit-cell dimensions

The unit-cell dimensions refined from powder X-ray diffraction data are a = 15.7313(3), c = 11.7623(3) Å, V = 2910.9(1) $Å^3$, and those refined from single-crystal X-ray diffraction data are a = 15.7250(4) and c = 11.7736(3) Å. Both sets of unit-cell dimensions plot close to the trend for boron-bearing vesuvianite on the graph of c versus a in Groat et al. (1992a) and very close to or just within the field defined for wiluite ($P4/nnc$) on the graph of c versus a in Gnos and Armbruster (2006) (see Fig. 2).

Crystal structure refinement

Data collection and refinement parameters for the single-crystal X-ray experiments are summarized in Table 2, positional and displacement parameters in Table 3, and bond lengths in Table 4.

The atom at the X1 site is coordinated by eight O atoms: four at O1 positions (at distances of 2.337 Å) and four at O2 sites (at distances of 2.508 Å). The mean X1–O distance is 2.423 Å and the refined site-occupancy and bond distances suggest that the X1 site is fully occupied by Ca. The atom at the X2 site is coordinated by eight O atoms at distances of 2.346 to 3.024 Å (mean 2.488 Å). The refined site-occupancy and bond distances suggest only Ca at the X2 site. The atom at the X3 position is coordinated by a plethora of anions at fully and partially occupied sites. The former include O atoms at the O3 and O6 positions and O, OH, and F atoms at the O11 site. The latter include O atoms at the O7A, O7B, O10, O12A, and O12B positions. The refined site occupancy suggests both Ca (0.962) and Fe (0.038) at the X3 site. The bond distances and valence suggest that the Fe is divalent. The atom at the X4 site is coordinated by eight O atoms, four at O6 sites (at distances of 2.333 Å) and four at O9 positions (at distances of 2.627 Å), for a mean X4–O distance of 2.480 Å.

The Y1 position is coordinated by four O atoms at the O6 site and one anion (O, OH, or F) at the O10 site. The Y1–O6 distances are 2.080 Å and the Y1–O10 distance is 2.267 Å. Previous studies have suggested that Fe orders preferentially at the Y1 position and that appears to be the case here. The mean Y1–φ (φ: unspecified anion) distance of 2.117 Å is similar to that reported in other studies for *P*4/*nnc* vesuvianite with an unsplit Y1 position completely occupied by Fe (e.g., 2.125 Å in Ohkawa et al. 1992; 2.055 Å in Ohkawa et al. 1994; 2.11 Å in Britvin et al. 2003; and 2.058, 2.078 and 2.078 Å in Galuskin et al. 2003). Bond-valence analysis suggests that the Fe at the Y1 site is predominantly divalent. Adjacent X4 and Y1 positions cannot both be occupied at the same time, and the refined site occupancies suggest that both Y1 and X4 are half occupied.

The atom at the Y2 site is coordinated by O atoms at two O4 (at distances of 1.935 Å), two O8 (at distances of 1.898 Å), and two O11 positions (at distances of 1.905 Å), and the mean Y2–O distance is 1.913. The refined site occupancies indicate that this site is occupied by Al (0.954) and As (0.046) and the bond distances and valences suggest that the latter is pentavalent.

The atom at the Y3 position is coordinated by six O atoms at distances of 1.947 to 2.084 Å (mean 2.018 Å). The refined site-occupancy suggests 0.618 (Al + Mg) and 0.382 Fe at the Y3 site. Bond-valence analysis suggests that the Fe at the Y3 site is trivalent.

The main effect of the unusually high Fe content of this sample is to increase the mean Y3–O distance which in vesuvianite is more typically in the range of 1.93-1.97 Å and is rarely over 2.00 Å. Previously, Fitzgerald et al. (1987) reported a mean Y3–O distance of 2.035 Å for a REE-bearing vesuvianite with 6.56 wt.% FeO (3.10 Fe pfu) from San Benito County in California, and Groat et al. (1996) described a mean Y3–O distance of 2.012 Å for the Fe-rich (3.71 wt.% FeO and 3.80 wt.% Fe_2O_3, corresponding to 1.59 Fe^{2+} and 1.46 Fe^{3+} pfu) wiluite from Tulare County in California.

The atom at the Z1 site is coordinated by four O atoms at the O1 site at distances of 1.636 Å. The bond distances and valences and refined site occupancies suggest that the Z1 position is fully occupied by Si. The atom at the Z2 site is coordinated by four O atoms at the O7 (at distances of 1.620 Å for O7A and 1.663 Å for O7B), O2 (at a distance of 1.640 Å), O3 (at a distance of 1.641 Å), and O4 (at a distance of 1.676 Å) sites. The mean Z2–O distances are 1.644 (O7A occupied) and 1.655 Å (O7B occupied). The bond distances and valences and refined site occupancy suggest that the Z2 site is occupied by Si (0.971) and some As (0.029). The atom at the Z3 site is coordinated by four O atoms at the O6 (1.611 Å), O5 (1.627 Å), O8 (1.630 Å), and O9 (1.6649 Å) positions, for a mean Z3–O distance of 1.633 Å. The bond distances and valences and refined site occupancy suggest that the Z3 position is fully occupied by Si. We note that refinement of the occupancies of the *Z* sites showed no evidence of the partial hydrogarnet-like substitution of SiO_4 tetrahedra by H_4O_4 described by Armbruster and Gnos (2000b).

The atom at the T1 site is coordinated by two anions (O, OH, or F) at the O11 sites (1.546 Å) and two O atoms at the O7B sites (1.59 Å) for mean T1–φ distance of 1.57 Å. These distances and the bond valences suggest that the T1 site contains B. Presumably this only happens when the O7B site is occupied; however the refined site-occupancy of the T1 position (0.42) is larger than that of O7B (0.39) which might suggest that another cation may also be present at the T1 position. However unlike in the Bi- and Mn-bearing vesuvianite described by Groat and Evans (2012), there is no evidence for As at the T1 site.

The atom at the T2 position is trigonally-coordinated by O atoms at the O10 position, at a distance of 1.306 Å, and two atoms at O12A positions, at distances of 1.28 Å. The distances, bond valences, and site occupancies suggest that the T2 site contains B, with a refined site occupancy of 0.90 apfu. However the total population of the O12A site is 0.65 apfu, which can coordinate only 0.65/2 = 0.32 B at T2 pfu; this leaves 0.58 apfu B to be coordinated in some other way. The T2-O12B distance of 1.68 Å is too long for trigonally-coordinated B, but it is possible to form a nearly equilateral triangle (with edges 2.34 Å, 2.34 Å, 2.32 Å) from one O10 and two O12B positions. The centre of this triangle (at 0.229, 0.206, 0.234) is 0.80 Å from the T2 position, and is 1.36 Å from O10 and 1.34 from O12B, which are acceptable trigonal B-O distances, and could correspond to the small lobes seen in the electron density map (Fig. 3). With a total population of the O12B site of 0.76 apfu, this type of coordination could account for 0.76/2 = 0.38 B pfu, which would require each lobe site to have an occupancy of 0.048. The O10-O12A-O12A and O10-O12B-O12B type of trigonal coordinations together consume 0.65 + 0.76 = 1.41 O10 pfu out of a total O10 occupancy of 1.64 apfu.

A possibility for the remaining O10 occupancy (0.23 apfu) is B at T2 in linear [2]-coordination with O atoms at two O10 positions, as suggested by Groat et al. (1996). However two-coordinate boron is unknown in minerals; it occurs rarely in synthetic chemical compounds, usually involving nitrogen as one or both coordinating ligands (Kölle and Nöth 1985, Piers et al. 2005). In addition, Raman spectra of randomly oriented vesuvianite crystals did not show features suggesting other than 3- and 4-fold boron coordination. Nevertheless, this coordination would contribute an additional 0.23/2 = 0.12 B pfu. These three coordination environments at or near T2 would thus account for 0.32+0.38+0.12 = 0.82 B pfu, close to the refined T2 population of 0.90 apfu.

The refined site occupancies of the O7A and O7B sites are 0.61 and 0.39, respectively. The O7A–O7B distance is 0.53 Å which is similar to the O7A–O7B distances of ~0.5 Å reported by Groat et al. (1994, 1996) for boron-bearing vesuvianite.

The atom at the O10 position (with occupancy 0.820) shows a large (U_{eq} = 0.039) but approximately spherical displacement ellipsoid. The atom at the O10 position is 1.26 Å from four O12A positions; 1.306 Å from a T2 site; 2.267 Å from a Y1 position; and 2.6212 Å from four X3 sites.

The atom at the fully occupied O11 position is 1.546 Å from a T1 site, 1.905 Å from a Y2 position, 2.000 Å from a Y3 site, and 2.507 Å from an X3 site.

The refined site occupancies of the O12A and O12B positions are 0.08 and 0.10, respectively, corresponding to total site populations of 0.65 O12A and 0.76 O12B apfu . The O12A–O12B distance is 0.63 Å. The atom at the O12A site is 1.28 Å from a T2 position, and 2.22, 2.24, and 2.81 Å from three X3 sites. The atom at the O12B position is 1.68 Å from the T2 site, 2.27 Å from one X3 site, and 2.28 Å from two other X3 positions. So the difference between O12A and O12B is that the latter is coordinated by three close X3 positions, not just two. Could this be related to the presence of Fe at X3? The radius of 8-coordinated Ca is 1.12 Å and that of 8-coordinated Fe^{2+} is 0.92 Å (Shannon 1976), so there is quite a size difference. We note that the X3 position is coordinated by two O12A and three O12B sites. Iron at X3 is 0.308 apfu and O12B is 0.764 apfu, and if if Fe at X3 is coordinated by a 2.5 O12B on average, that would account for all the O12B.

The T2 site cannot have the O10-O12A-O12A coordination (which accounts for a maximum 0.32 apfu B at T2) or the linear O10-O10 coordination (maximum 0.12 apfu B at T2) when any O12B positions is occupied. Therefore when the nearby X3 site contains Fe the T2 position is either vacant (0.102 apfu) or the B at T2 must be [3]-coordinated by some combination involving an O10 and at least one O12B site (probably two), in which case the B atom would likely sit off of the T2 site to reduce the B-O12B distance.

Mössbauer spectroscopy

A room-temperature Mössbauer spectrum obtained from the vesuvianite sample is shown in Figure 4, and the hyperfine parameters for a three Lorentz doublet model along with doublet assignments based on the crystal structure refinement, are given in Table 5. The doublet with high quadrupole splitting (black in Fig. 4) with 5% area (compared to 7% abundance from the site refinement data) corresponds to Fe^{2+} at the X3 position. Its hyperfine parameters are characteristic of Fe^{2+} in [6]- or higher coordination. The broad doublet (dark grey in Fig. 4) with 17% area (compared to 23% abundance from the site refinement data) most likely corresponds to Fe^{2+} at the Y1 site. Although its associated mean centre shift and quadrupole splitting are low for Fe^{2+} (compare values for the X3 doublet), this and the broad line-width are characteristic for a

Fe^{2+}-occupied site with significant static disorder in its local environment (Evans 2006), as is expected for Y1 due to its unusual coordination and proximity to several partially occupied and/or substituted sites. The strongest doublet (light grey in Fig. 4) with 78% area (compared to 70% abundance from the structure refinement) has hyperfine parameters characteristic of octahedrally-coordinated Fe^{3+}, and almost certainly corresponds to Fe^{3+} at the Y3 site. There is no need to assign any of the Mössbauer absorption to Fe^{2+}-Fe^{3+} electron transfer (although a small amount, perhaps a maximum of 10%, cannot be ruled out). The Fe^{3+}/Fe ratio based on the above interpretation is 0.78(4).

DISCUSSION

The average electron microprobe composition and the composition from the site refinement result in the following formulae:

$Ca_{18.45}(Fe_{4.66}Mn_{0.06})_{\Sigma 4.72}(Al_{5.31}Mg_{3.36})_{\Sigma 8.67}As_{0.46}Si_{17.65}B_{2.45}(O_{75.88}F_{2.26})_{\Sigma 78.14}$ (EMPA)

$Ca_{18.69}(Fe, Mn)_{\Sigma 4.37}(Al, Mg)_{\Sigma 8.76}As_{0.42}Si_{17.77}B_{2.60}(O,OH,F)_{\Sigma 79.02}$ (SREF)

The formulae are similar. Boron in the composition from the site refinement is slightly more than the amount needed for wiluite (2.50 apfu; Groat et al. 1998) and that in the average electron microprobe composition is only slightly less. The individual electron microprobe compositions confirm that some areas of the structure crystal do contain enough B to be classified as wiluite.

The formulae are also similar for Fe which as noted previously is the highest concentration ever recorded from vesuvianite. The site refinement and Mössbauer results confirm Fe^{2+} at the X3 and Y1 sites and Fe^{3+} at the Y3 position. Most of the Fe (70% from the site refinements and 78% from the Mössbauer interpretation) is ferric.

The As compositions are also similar (0.46 As apfu in the average electron microprobe composition and 0.42 As apfu from the site refinements). The As substituting for Si at the tetrahedrally coordinated Z2 position is most likely pentavalent given the ionic radius of 0.335 for $^{IV}As^{5+}$ compared to 0.26 for ^{IV}Si (Shannon 1976). The As substituting for Al at the Y2 position is interesting for a number of reasons, not least because in almost all reported

vesuvianite crystal structures the Y2 site is completely occupied by Al. This arsenic is also probably pentavalent given that As^{3+} generally exhibits a lone pair of electrons which is not evident here. Arsenic in octahedral coordination is also very rare; according to Schwendtner and Kolitsch (2007) there are more than 900 crystal structures (with conventional *R* factor < 0.072, no partial substitution of the As or O atoms) with AsO_4 polyhedra in the International Crystal Structure Database, but only 33 with AsO_6 polyhedra, therefore AsO_6 polyhedra occur in less than 3% of all arsenates. Schwendtner and Kolitsch (2007) also reported that the mean As-O distance in these 33 polyhedra is 1.830(2) Å, which is much shorter than our average Y2–O distance of 1.913 Å, but then As only comprises ~4% of the site contents. A bond length of 1.915 Å was calculated using the ionic radii of Shannon (1976) of 0.54 Å for $^{VI}Al^{3+}$, 0.46 Å for $^{VI}As^{5+}$, 1.36 Å for $^{III}O^{2-}$, and 1.38 Å for $^{IV}O^{2-}$, weighted by the occupancies of Y2 and T1 (to account for variable coordination of O11), in good agreement with the average Y2–O distance of 1.913 Å. Groat and Evans (2012) found As at the T1 site in a vesuvianite sample from Långban in Sweden, but there is no evidence for that here. This is likely due to the presence of B at the T1 site, which is absent in the sample from Långban.

What about F? The average electron microprobe composition shows 2.26 F apfu which is very high for B-bearing vesuvianite or wiluite. Groat et al. (1992b) showed that F substitutes for OH at both the O10 and O11 sites in the vesuvianite structure but given that the T2 position is almost completely (90%) occupied by B it is unlikely that there is any substantial amount of F or OH at the O10 site. It is much more likely that F and OH are concentrated at the O11 position when the T1 site is vacant.

The occupancy of the Y3 position refined to 0.618 (Mg + Al) and 0.382 Fe^{3+}. The average electron microprobe composition shows 3.36 Mg pfu, and assuming that all of the Mg is at the Y3 position the occupancy of the site is 0.420 Mg, 0.382 Fe^{3+}, and 0.198 Al. The occupancy of the T1 position refined to 0.43 B, similar to Mg at Y3, as required by the substitutional vector $MgBAl_{-1}H_{-2}$ introduced by Groat et al. (1992a, 1994). Occupancy of T1 by B and Y3 by Mg would seem to neccessitate O at O11 and O7B (refined occupancy 0.39).

The average electron microprobe composition also shows 2.26 F pfu and the assumption we have made is that this substitutes at O11 along with OH. Since we need 0.43 O at O11 to balance B at T1 and we have 0.28 F we can have a maximum of approximately 0.29 OH at O11. However Figure 9 in Bellatreccia et al. (2005b), which shows the relationship between the OH

content apfu determined by secondary-ion mass-spectrometry (SIMS) or Fourier-transform infrared (FTIR) versus Mg (EMPA) for boron-bearing vesuvianite, suggests approximately 1.3 OH pfu, or a maximum of 0.16 OH at O11. This would mean that the occupancy of the O11 site is 0.56 O, 0.28 F, and 0.16 OH.

The *P*4/*nnc* symmetry indicates that this vesuvianite formed at high temperatures (400-800 ºC) and the predominance of ferric iron and pentavalent arsenic suggests under oxidizing conditions.

The results showing Fe at three different sites with three different coordinations attests to the flexibility of the vesuvianite crystal structure. The incorporation of As at two different sites in the structure shows that rock-forming silicate minerals such as vesuvianite (or, e.g., the dumortierite-group minerals; see Groat et al. 2009, 2012) can be a reservoir for this heavy element.

ACKNOWLEDGEMENTS

The authors thank M. Raudsepp for the unit-cell dimensions refined from X-ray powder diffraction data. We also thank J Engelbrecht for helping prepare the manuscript which was improved by comments from M. Parker, U. Halenius, an anonymous reviewer, Associate Editor G. Diego Gatta, and the Editor. Financial support was provided by the Natural Sciences and Engineering Research Council of Canada in the form of a Discovery Grant to LAG. and by GACR (project GAP210/10/0743) to SH.

435 **REFERENCES**

436

437 Allen, F.M. and Burnham, C.W. (1992) A comprehensive structure-model for vesuvianite:
438 Symmetry variations and crystal growth. Canadian Mineralogist, 30, 1-18.
439
440 Armbruster, T. and Gnos, E. (2000a) *P*4/*n* and *P*4*nc* long-range ordering in low-temperature
441 vesuvianites. American Mineralogist, 85, 563-569.
442
443 Armbruster, T. and Gnos, E. (2000b) Tetrahedral vacancies and cation ordering in low-
444 temperature Mn-bearing vesuvianites: Indication of a hydrogarnet-like substitution.
445 American Mineralogist, 85, 570–577.
446
447 Azavant, P. and Lichanot, A. (1993) X-ray scattering factors of oxygen and sulfur ions: An ab
448 initio Hartree-Fock calculation. Acta Crystallographica A49, 91-97.
449
450 Bellatreccia, F., Camara, F., Ottolini, L., Della Ventura, G., Cibin, G., and Mottana, A. (2005a)
451 Wiluite from Ariccia, Latium, Italy: Occurrence and crystal structure. Canadian
452 Mineralogist, 43, 1457-1468.
453
454 Bellatreccia, F., Della Ventura, G., Ottolini, L., Libowitzky, E., and Beran, A. (2005b) The
455 quantitative analysis of OH in vesuvianite: a polarized FTIR and SIMS study. Physics and
456 Chemistry of Mineral, 32, 65-76.
457
458 Britvin, S.N., Antonov, A.A., Krivovichev, S.V., Armbruster, T., Burns, P.C., and Chukanov, N.V.
459 (2003) Fluorvesuvianite, $Ca_{19}(Al,Mg,Fe^{2+})_{13}[SiO_4]_{10}[Si_2O_7]_4O(F,OH)_9$, a new mineral
460 species from Pitkäranta, Karelia, Russia: Description and crystal structure. Canadian
461 Mineralogist, 41, 1371-1380.
462
463 Bruker (2007) *SAINT*. Bruker AXS Inc., Madison, Wisconsin, USA.
464

Creagh, D.C. and Hubbell, J.H. (1992) International Tables for Crystallography, Vol C. Kluwer Academic Publishers, Boston, 200–206.

Creagh, D.C. and McAuley, W.J. (1992) International Tables for Crystallography, Vol C. Kluwer Academic Publishers, Boston, 219–222.

Cromer, D.T. and Waber, J.T. (1974) International Tables for X-ray Crystallography, Vol. IV. The Kynoch Press, Birmingham, England.

Eby, R.K., Janeczek, J., Ewing, R.C., Ercit, T.S., Groat, L.A., Chakoumakos, B.C., Hawthorne, F.C., and Rossman, G.R. (1993) Metamict and chemically altered vesuvianite. Canadian Mineralogist, 31, 357-369.

Evans, R. J. (2006) Mössbauer hyperfine parameters in oxygen-coordinated octahedral Fe^{2+} from electric structure calculations. Ph.D. Thesis, University of Ottawa, Ottawa, Ontario, Canada.

Fitzgerald, S., Rheingold, A.L., and Leavens, P.B. (1986) Crystal structure of a non-*P*4/*nnc* vesuvianite from Asbestos, Quebec. American Mineralogist, 71, 1483-1488.

Fitzgerald, S., Leavens, P.B., Rheingold, A.L., and Nelen, J.A. (1987) Crystal structure of a REE-bearing vesuvianite from San Benito County, California. American Mineralogist, 72, 625-628.

Fitzgerald, S., Leavens, P.B., and Nelen, J.A. (1992) Chemical variation in vesuvianite. Mineralogy and Petrology, 46, 163-178.

Galuskin, E.V., Armbruster, T., Malsy, A., Galuskina, I.O., and Sitarz, M. (2003) Morphology, composition and structure of low-temprature *P*4/*nnc* high-fluorine vesuvianite whiskrs from polar Yakutia, Russia. Canadian Mineralogist, 41, 843-856.

Giuseppetti, G. and Mazzi, F. (1983) The crystal structure of a vesuvianite with *P*4/*n* symmetry. Tschermaks Mineralogische und Petrographische Mitteilungen, 31, 277-288.

Gnos, E. and Armbruster, T. (2006) Relationship among metamorphic grade, vesuvianite "rod polytypism," and vesuvianite composition. American Mineralogist, 91, 862–870.

Groat, L.A. and Evans, R.J. (2012) Crystal chemistry of Bi- and Mn-bearing vesuvianite from Långban, Sweden. American Mineralogist, 97, 1627-1634.

Groat, L.A., Evans, R.J., Grew, E.S., Pieczka and Ercit, T.S. (2009) The crystal chemistry of holtite. Mineralogical Magazine, 73, 1033-1050.

Groat, L.A., Evans, R.J., Grew, E.S., and Pieczka, A. (2012) Crystal chemistry of As- and Sb-bearing dumortierite. Canadian Mineralogist, 50, 855-872.

Groat, L.A., Hawthorne, F.C., and Ercit, T.S. (1992a) The chemistry of vesuvianite. Canadian Mineralogist, 30, 19–48.

Groat, L.A., Hawthorne, F.C., and Ercit, T.S. (1992b) The role of fluorine in vesuvianite: a crystal-structure study. Canadian Mineralogist, 30, 1065-1075.

Groat, L.A., Hawthorne, F.C., and Ercit, T.S. (1994) The incorporation of boron into the vesuvianite structure. Canadian Mineralogist, 32, 505–523.

Groat, L.A., Hawthorne, F.C., Lager, G.A., Schultz, A.J., and Ercit, T.S. (1996) X-ray and neutron crystal-structure refinements of a boron-bearing vesuvianite. Canadian Mineralogist, 34, 1059–1070.

Groat, L.A., Hawthorne, F.C., Ercit, T.S., and Grice, J.D. (1998) Wiluite, $Ca_{19}(Al,Mg,Fe,Ti)_{13}(B,Al,\square)_5Si_{18}O_{68}(O,OH)_{10}$, a new mineral species isostructural with

vesuvianite, from the Sakha Republic, Russian Federation. Canadian Mineralogist, 36, 1301–1304.

Holland, T.J.B and Redfern, S.A.T. (1997) Unit cell refinement from powder diffraction data: the use of regression diagnostics. Mineralogical Magazine, 61, 65-77.

Hrazdil, V., Houzar, S. and Škoda, R. (2009) Sn-rich, As-vesuvianite bearing mineral assemblage from Nedvědice Marble at Kozlov, West Moravia, Svratka Crystalline Complex (A preliminary report). Geol. Výzk. Mor. Slez., Brno 2009, 109-113.

Hrazdil, V., Houzar, S., Cempírek, J. (2011) Tin-bearing skarns with As mineralization at the south-eastern margin of the Bohemian Massif. Mineralogical Magazine, 75, 1052.

Ibers, J.A. and Hamilton, W.C. (1964) Dispersion corrections and crystal structure refinements. Acta Crystallographica, 17, 781–782.

Kölle, P., and Nöth, H. (1985) The chemistry of borinium and borenium ions. Chemical Reviews, 85, 399-418.

Momma, K. and Izumi, F. (2011) VESTA 3 for three-dimensional visualization of crystal, volumetric and morphology data. Journal of Applied Crystallography, 44, 1272-1276.

Ohkawa, M., Yoshiasa, A., and Takeno, S. (1992) Crystal chemistry of vesuvianite: Site-preferences of square-pyramidal coordinated sites. American Mineralogist, 77, 945-953.

Ohkawa, M., Yoshiasa, A., and Takeno, S. (1994) Structural investigation of high- and low-symmetry vesuvianite. Mineralogical Journal, 17, 1-20.

Pan, Y. and Fleet, M.E. (1992) Mineral chemistry and geochemistry of vanadian silicates in the Hemlo gold deposit, Ontario, Canada. Contributions to Mineralogy and Petrology, 109, 511-525.

Pavese, A., Principe, M., Tribaudino, M., and Aagaard, St. S. (1998) X-ray and neutron single-crystal study of *P*4/*n* vesuvianite. Canadian Mineralogist, 36, 1029-1037.

Petricek, V., Dusek, M., and Palatinus L. (2006) Jana2006. Structure Determination Software Programs. Institute of Physics, Praha, Czech Republic.

Piers, W.E., Bourke, S.C., and Conroy, K.D. (2005) Borinium, borenium, and boronium ions: synthesis, reactivity, and applications. Angewandte Chemie International Edition 44, 5016-5036.

Pouchou, J.-L. and Pichoir, F. (1985) PAP $\phi(\rho Z)$ procedure for improved quantitative microanalysis. In: Armstrong, J.T. (ed.) Microbeam Analysis. San Francisco Press Inc., San Francisco, 104-106.

Prescher, C., McCammon, C., and Dubrovinsky, L. (2012) MossA - a program for analyzing energy-domain Mossbauer spectra from conventional and synchrotron sources. Journal of Applied Crystallography, 45, 329-331.

Schwendtner, K. and Kolitsch, U. (2007) Octahedral As in *M*+ arsenates – architecture and seven new members. Acta Crystallographica, B63, 205-215.

Shannon, R.D. (1976) Revised effective ionic radii and systematic studies of interatomic distances in halides and chalcogenides. Acta Crystallographica, A32, 751-767.

Sheldrick, G. M. (1996) *SADABS*. University of Göttingen, Germany.

Sheldrick, G. M. (2008) A short history of SHELX. Acta Crystallographica, A64, 112-122.

586 Yoshiasa, A. and Matsumoto, T. (1986) The crystal structure of vesuvianite from Nakatatsu mine:
587 Reinvestigation of the cation site-populations and of the hydroxyl groups. Mineralogical
588 Journal, 13, 1-12.
589
590 Young, R.A., Sakthivel, A., Moss, T.S. and Paiva-Santos, C.O. (1995) DBWS9411 - an upgrade
591 of the DBWS*.* programs for Rietveld refinement with PC and mainframe computers.
592 Journal of Applied Crystallography, 28, 366-367.

FIGURE CAPTIONS

FIG. 1. (a) Projection of the vesuvianite structure down [100]; (b) projection of the vesuvianite structure down [001].

FIG. 2. Unit cell parameters (square, from powder data; circle, from single-crystal data) plotted on the graph of *a* vs. *c* with regions from Figure 3 of Gnos and Armbruster (2006). The error bars are smaller than the symbols.

FIG. 3. Observed electron density around T2, O12A and O12B sites (isosurfaces are for an electron density of 2.5).

FIG. 4. Room temperature Mössbauer spectrum of the vesuvianite sample. The doublets are shaded as follows: Fe^{3+} Y3 - light grey, Fe^{2+} Y1 – dark grey, Fe^{2+} X3 – black. The fit residual is shown above the spectrum.

TABLE 1. Electron microprobe compositions

	1	2	3	4	5	Average	σ
As_2O_5 (wt.%)	1.73	1.62	1.75	1.68	1.78	1.71	0.06
SiO_2	34.69	34.97	34.32	34.43	34.02	34.49	0.32
SnO_2	0.09	0.12	0.08	0.09	0.08	0.09	0.01
B_2O_3	3.06	3.40	2.25	2.54	2.62	2.77	0.41
Al_2O_3	8.98	9.00	8.66	8.74	8.67	8.81	0.15
Fe_2O_3	12.19	12.30	11.95	11.92	12.14	12.10	0.14
MgO	4.54	4.55	4.36	4.33	4.23	4.40	0.12
CaO	33.69	33.52	33.53	33.94	33.61	33.66	0.15
MnO	0.12	0.15	0.13	0.11	0.13	0.13	0.01
ZnO	0.10	0.14	0.08	0.11	0.12	0.11	0.02
F	1.37	1.39	1.40	1.38	1.44	1.40	0.02
O=F	-0.58	-0.59	-0.59	-0.58	-0.61	-0.59	0.01
Total	99.98	100.57	97.92	98.69	98.23	99.08	1.02
As^{5+} (*apfu*)	0.459	0.429	0.471	0.450	0.480	0.458	0.018
Si^{4+}	17.622	17.723	17.680	17.637	17.563	17.645	0.054
Sn^{4+}	0.018	0.024	0.016	0.018	0.016	0.018	0.003
B^{3+*}	2.683	2.974	2.001	2.246	2.335	2.448	0.342
Al^{3+}	5.376	5.376	5.258	5.276	5.275	5.312	0.052
Fe^{3+}	4.660	4.691	4.632	4.595	4.716	4.659	0.043
Mg^{2+}	3.438	3.438	3.348	3.307	3.255	3.357	0.072
Ca^{2+}	18.337	18.202	18.507	18.628	18.591	18.453	0.161
Mn^{2+}	0.052	0.064	0.057	0.048	0.057	0.056	0.005
Zn^{2+}	0.038	0.052	0.030	0.042	0.046	0.042	0.007
F^-	2.201	2.228	2.281	2.236	2.351	2.259	0.053
O^{2-}	76.272	76.772	75.209	75.516	75.622	75.878	0.565

Note: Compositions normalized on 50 cations (less B).

TABLE 2. Data measurement and refinement information

a (Å)	15.7250(4)
c (Å)	11.7736(3)
V (Å^3)	2911.3(1)
Space group	*P*4/*nnc*
Z	4
Crystal size (mm)	0.15 × 0.15 × 0.10
Radiation	Mo*K*α
Monochromator	graphite
Total F_o	42562
Unique F_o	2785
$F_o > 4\sigma F_o$	2303
R_{int}	0.04(2)
L.s. parameters	187
Range of *h*	-23 ≤ 24
Range of *k*	-20 ≤ 24
Range of *l*	-16 ≤ 18
R_1 for $F_o > 4\sigma F_o$	0.0221
R_1 for all unique F_o	0.0337
wR_2	0.0546
a	0.0201
b	3.07
GooF (= *S*)	1.073
$\Delta\rho_{max}$ (e Å^{-3})	0.55
$\Delta\rho_{min}$ (e Å^{-3})	-0.69

$w = 1/[\sigma^2(F_o^2) + (a \times P)^2 + b \times P]$ where $P = [\text{Max}(F_o^2, 0) + 2 \times F_c^2)]/3$

TABLE 3. Positional and displacement parameters

Site	Multiplicity	*x/a*	*y/b*	*z/c*	U_{eq} (Å^2)	Population
X1	2	¾	¼	¼	0.0107(1)	1 Ca
X2	8	0.80992(2)	0.04456(2)	0.37968(3)	0.01080(7)	1 Ca
X3	8	0.89867(2)	-0.17887(2)	0.89420(3)	0.0198(1)	0.962(4) Ca + 0.038 Fe^{2+}
X4	2	¾	¾	0.1438(1)	0.0116(2)	0.5 Ca
Y1	2	¾	¾	0.0535(1)	0.0195(2)	0.5 Fe^{2+}
Y2	4	0	0	0	0.0105(2)	0.954(2) Al + 0.046 As^{5+}
Y3	8	0.88820(2)	0.12073(2)	0.12770(3)	0.0094(1)	0.618(3) Al + 0.382 Fe^{3+}
Z1	2	¾	¼	0	0.0079(1)	1 Si
Z2	8	0.82162(3)	0.04056(3)	0.87099(3)	0.0099(1)	0.971(2) Si + 0.029 As^{3+}
Z3	8	0.91603(3)	0.84973(3)	0.36435(4)	0.00874(8)	1 Si
T1	4	0.0537(3)	0.0537(3)	¼	0.023(2)	0.42(2) B
T2	1	¼	¼	¼	0.038(3)	0.90(4) B
O1	8	0.77864(7)	0.17274(7)	0.0848(1)	0.0106(2)	1 O
O2	8	0.88004(7)	0.16113(7)	0.2836(1)	0.0120(2)	1 O
O3	8	0.95692(8)	0.22493(7)	0.0767(1)	0.0147(2)	1 O
O4	8	0.93910(7)	0.10456(7)	0.4700(1)	0.0112(2)	1 O
O5	8	0.82861(7)	0.01162(7)	0.1804(1)	0.0113(2)	1 O
O6	8	0.87975(8)	0.72413(7)	0.0542(1)	0.0150(2)	1 O
O7A	8	0.8237(9)	0.9446(3)	0.8211(6)	0.016(1)	0.61(4) O
O7B	8	0.854(2)	0.9530(6)	0.8044(9)	0.019(2)	0.39(4) O
O8	8	0.93977(7)	0.90858(7)	0.0678(1)	0.0108(2)	1 O
O9	4	0.85388(7)	0.85388(7)	¼	0.0112(4)	1 O
O10	2	¾	¾	0.8609(4)	0.039(1)	0.82(1) O
O11	8	-0.00083(7)	0.05937(7)	0.1411(1)	0.0149(2)	1 O
O12A	8	0.185(2)	0.226(2)	0.307(2)	0.036(8)	0.08(1) O
O12B	8	0.152(2)	0.215(1)	0.281(2)	0.032(6)	0.10(1) O

TABLE 4. Selected interatomic distances (Å)

X1–O1	x4	2.337(1)	Y1–O6	x4	2.080(1)
X1–O2	x4	2.508(1)	Y1–O10[k]		2.267(5)
<X1–O>		2.423	<Y1–O>		2.117
X2–O8[a]		2.346(1)	Y2–O8[l]	x2	1.898(1)
X2–O5[b]		2.348(1)	Y2–O11	x2	1.905(1)
X2–O3[c]		2.384(1)	Y2–O4[m]	x2	1.935(1)
X2–O2		2.420(1)	<Y2–O>		1.913
X2–O5		2.420(1)			
X2–O4		2.480(1)	Y3–O2		1.947(1)
X2–O1[b]		2.486(1)	Y3–O1		1.973(1)
X2–O6[a]		3.024(1)	Y3–O11[n]		2.000(1)
<X2–O>		2.488	Y3–O5		2.051(1)
			Y3–O3		2.053(1)
X3–O3[d]		2.408(1)	Y3–O4[o]		2.084(1)
X3–O7A[e]		2.429(4)	<Y3–O>		2.018
X3–O7B[e]		2.433(6)			
X3–O6[f]		2.442(1)	Z1–O1	x4	1.636(1)
X3–O11[g]		2.507(1)			
X3–O7B[h]		2.542(5)	Z2–O7A[e]		1.620(3)
X3–O8[f]		2.547(1)	Z2–O3[p]		1.641(1)
X3–O7A[i]		2.54(2)	Z2–O2[c]		1.640(1)
X3–O10[e]		2.6212(7)	Z2–O7B[e]		1.663(8)
X3–O7A[h]		2.635(6)	Z2–O4[c]		1.676(1)
X3–O6[j]		2.851(1)	<Z2–O, O7A>		1.644
X3–O7B[i]		3.07(3)	<Z2–O, O7B>		1.655
<X3–O, O7A>		2.55			
<X3–O, O7B>		2.60	Z3–O6[q]		1.611(1)
			Z3–O5[r]		1.627(1)
X4–O6	x4	2.333(1)	Z3–O8[s]		1.630(1)
X4–O9	x4	2.627(2)	Z3–O9		1.6649(7)
<X4–O>		2.480	<Z3–O>		1.633

X3–O12A[u]	2.22(2)	T1–O11	x2	1.546(3)
X3–O12A[v]	2.24(2)	T1–O7B[o]	x2	1.59(3)
X3–O12B[u]	2.27(2)	<T1–O>		1.57
X3–O12B[g]	2.28(3)			
X3–O12B[v]	2.28(2)	T2–O12A	x2	1.28(3)
X3–O12A[g]	2.82(4)	T2–O10[t]		1.306(4)
		<T2–O>		1.29
X4–Y1	1.063(2)			
		T2–O12B	x2	1.68(3)
O7A–O7B	0.53(1)			
O12A–O12B	0.63(3)			

Note: a: *y*, *x* - 1, -*z* + ½ ; b: -*x* +3/2, *y*, -*z* + ½; c: -*y* + 1, -*x* + 1, *z* + ½; d: -*x* + 2, -*y*, -*z* + 1; e: *x*, *y* - 1, *z*; f: *x*, *y* - 1, *z* + 1; g: -*x* + 1, -*y*, -*z* + 1; h: *y*, *x* - 1, -*z* + 3/2; i: *y*, -*x* + ½, *z*; j: -*y* + 3/2, *x* - 1, *z* + 1; k: *x*, *y*, *z* - 1; l: -*x* + 1, -*y* + 1, -*z*; m: -*y*, -*x* + 1, *z* - ½; n: *x* + 1, *y*, *z*; o: -*y* + 1, -*x* + 1, *z* - ½; p: *y* + ½, -*x* + 1, -*z* + 1; q: *x*, -*y* + 3/2, -*z* + ½; r: *y* + 1, *x*, -*z* + ½; s: *y*, *x*, -*z* + ½; t: *x* - ½, -*y* + 1, *z* - ½; u: -*y* + 1, -*x*, *z* + ½; v: -*x* + 1, *y* - ½, *z* + ½.

TABLE 5. Lorentz-doublet fitting parameters of the room-temperature Mössbauer spectrum with Fe site assignments.

Fe^{3+} at ^{VI}Y3 (light grey doublet)	
Centre shift*	0.39(1) mm/s
Quadrupole splitting	0.53(1) mm/s
FWHM	0.44(1) mm/s
Area	78(4) %
Fe^{2+} at ^{VIII}X3 (black doublet)	
Centre shift*	1.15(2) mm/s
Quadrupole splitting	2.68(5) mm/s
FWHM	0.28(9) mm/s
Area	5(2) %
Fe^{2+} at ^{V}Y1 (dark grey doublet)	
Centre shift*	0.9(1) mm/s
Quadrupole splitting	1.2(2) mm/s
FWHM	1.4(5) mm/s
Area	17(4) %
Fe3+/ΣFe	**0.78(4)**

* relative to α-Fe

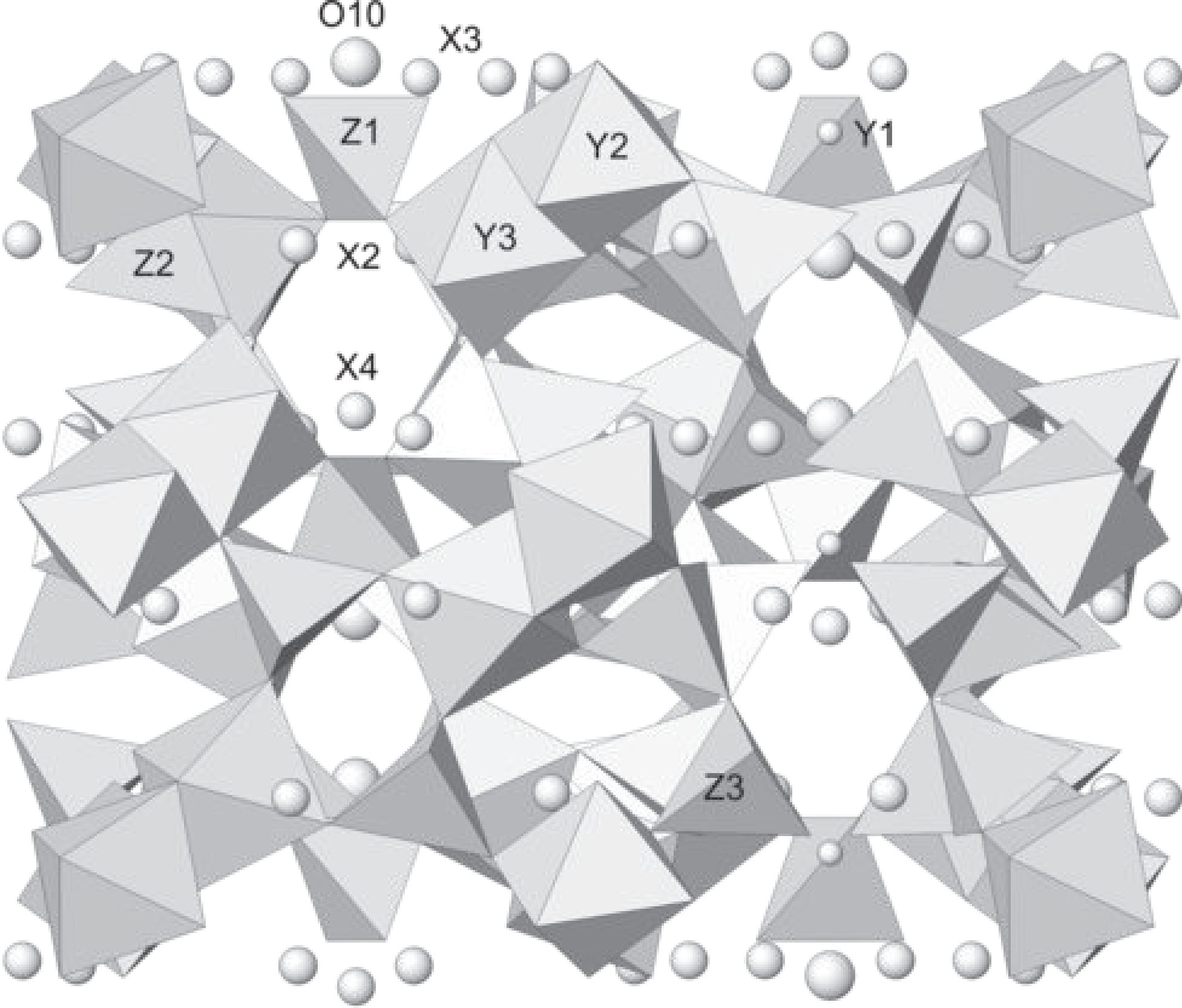

Fig. 1a

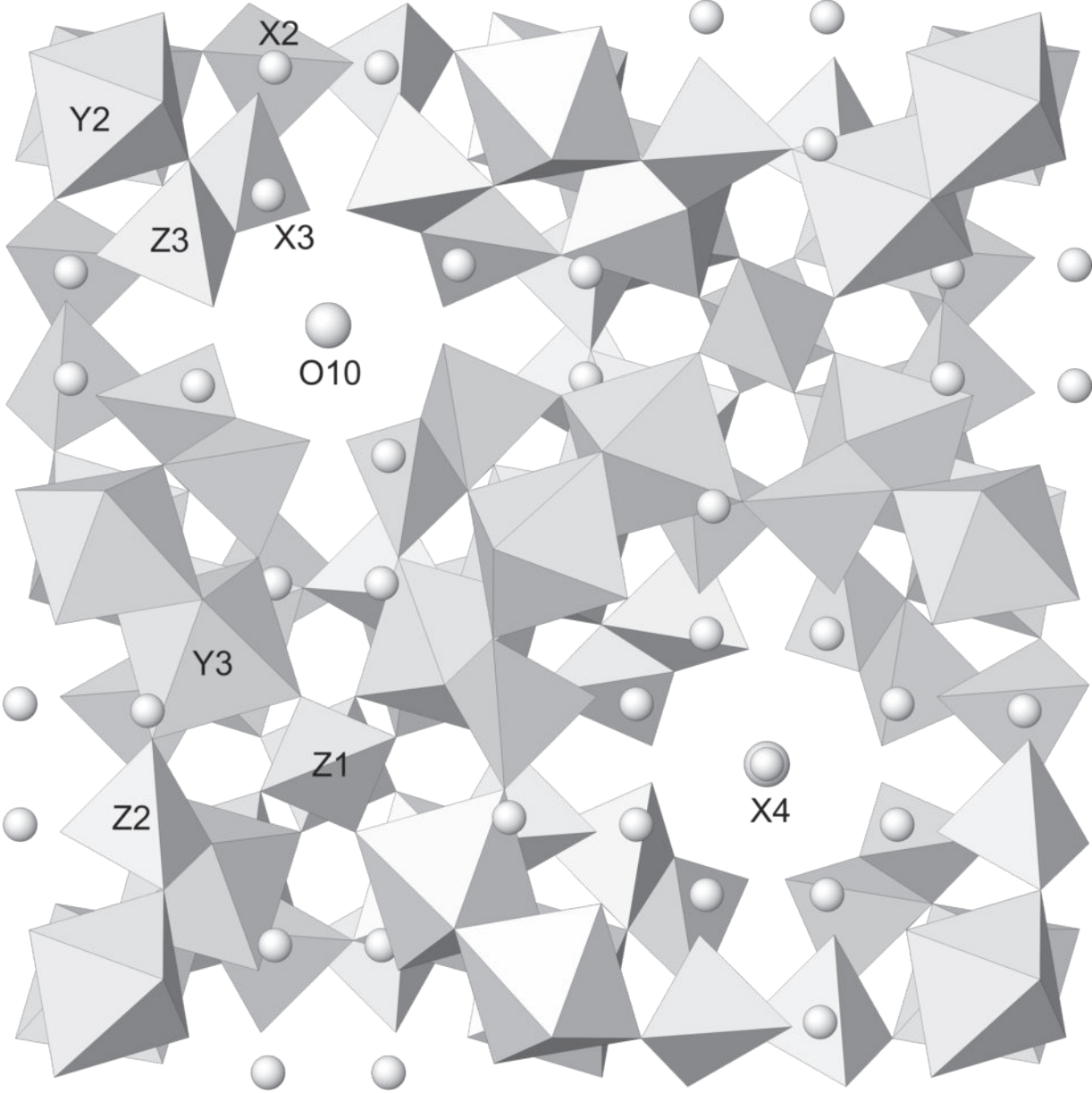

Fig. 1b

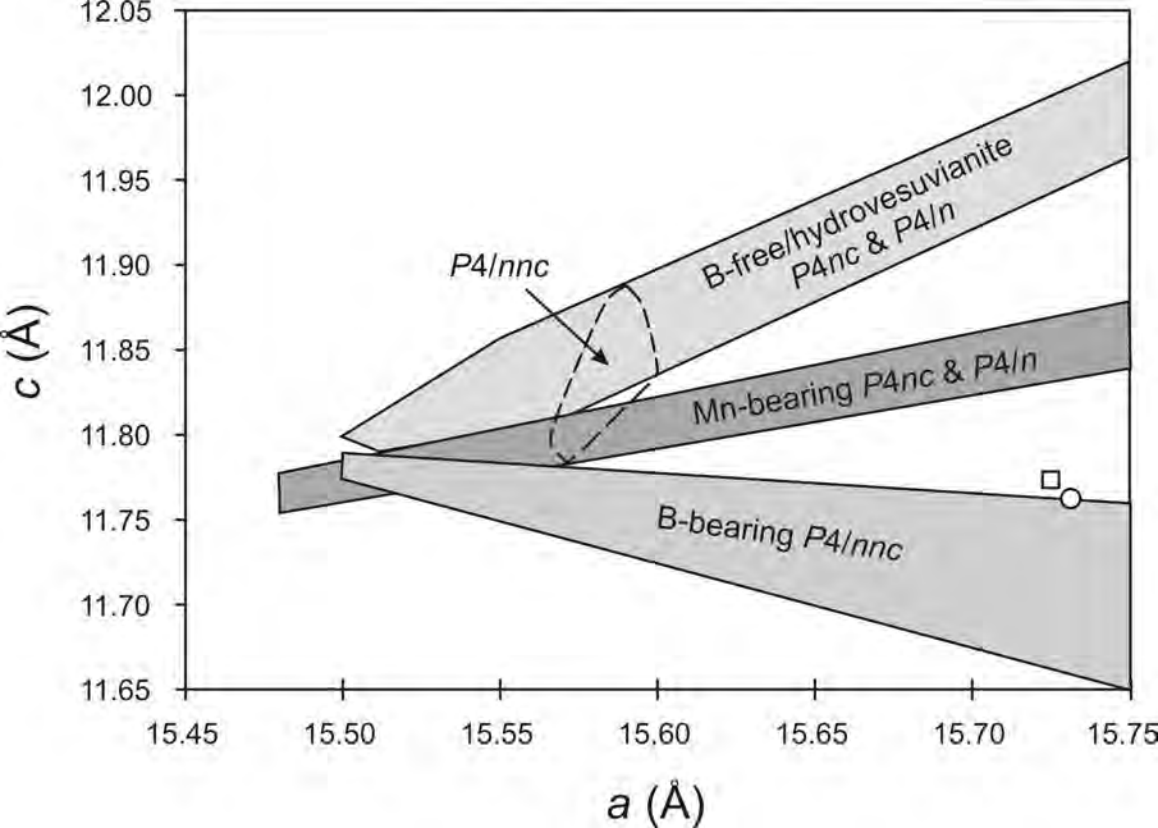
12.05
12.00
11.95
11.90
11.85
11.80
11.75
11.70
11.65
c (Å)
15.45
15.50
15.55
15.60
15.65
15.70
15.75
a (Å)
P4/nnc
B-free/hydrovesuvianite
P4nc & P4/n
Mn-bearing P4nc & P4/n
B-bearing P4/nnc

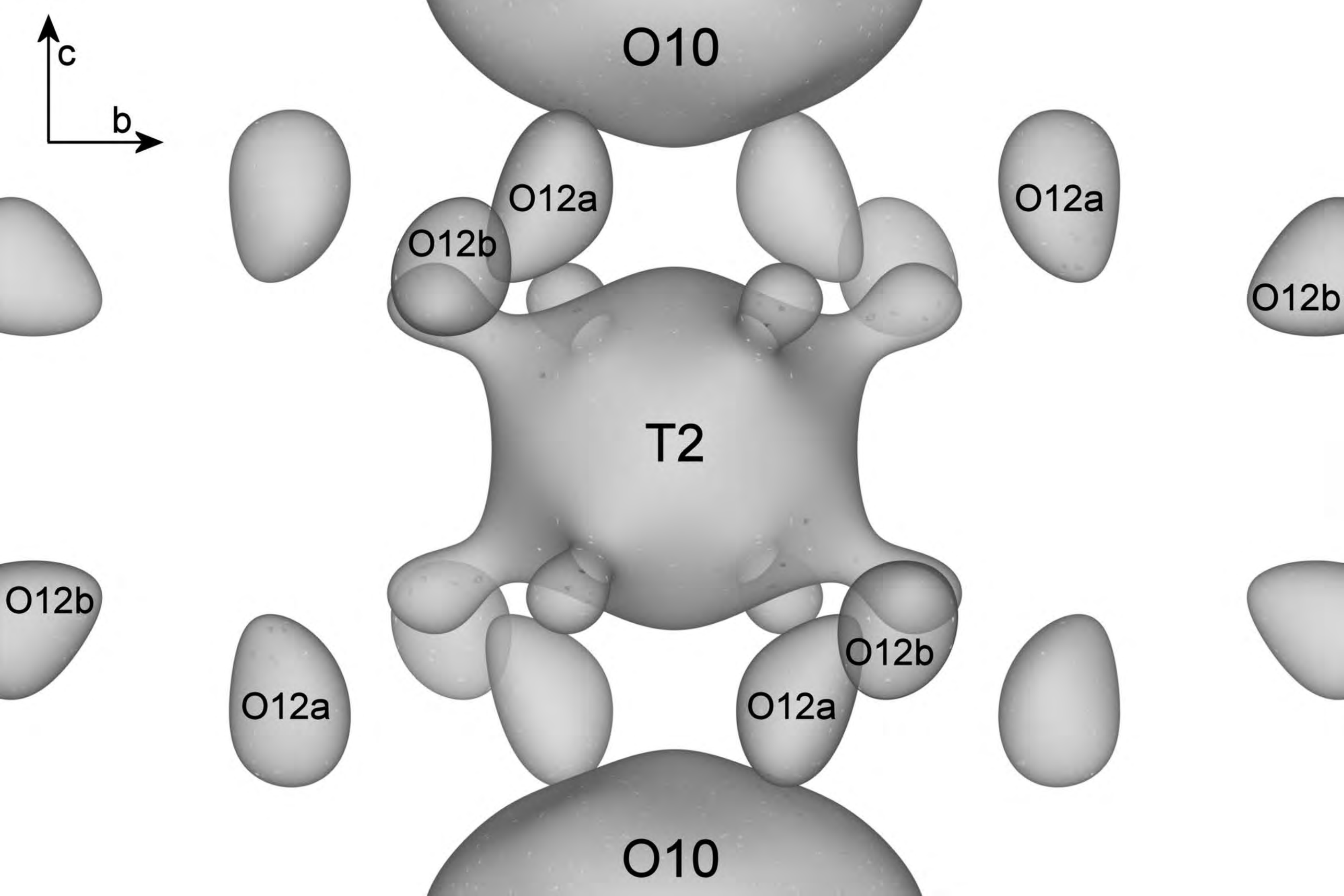
c
b
O10
O12a
O12b
T2
O12a
O12b
O12b
O12a
O12a
O12b
O10

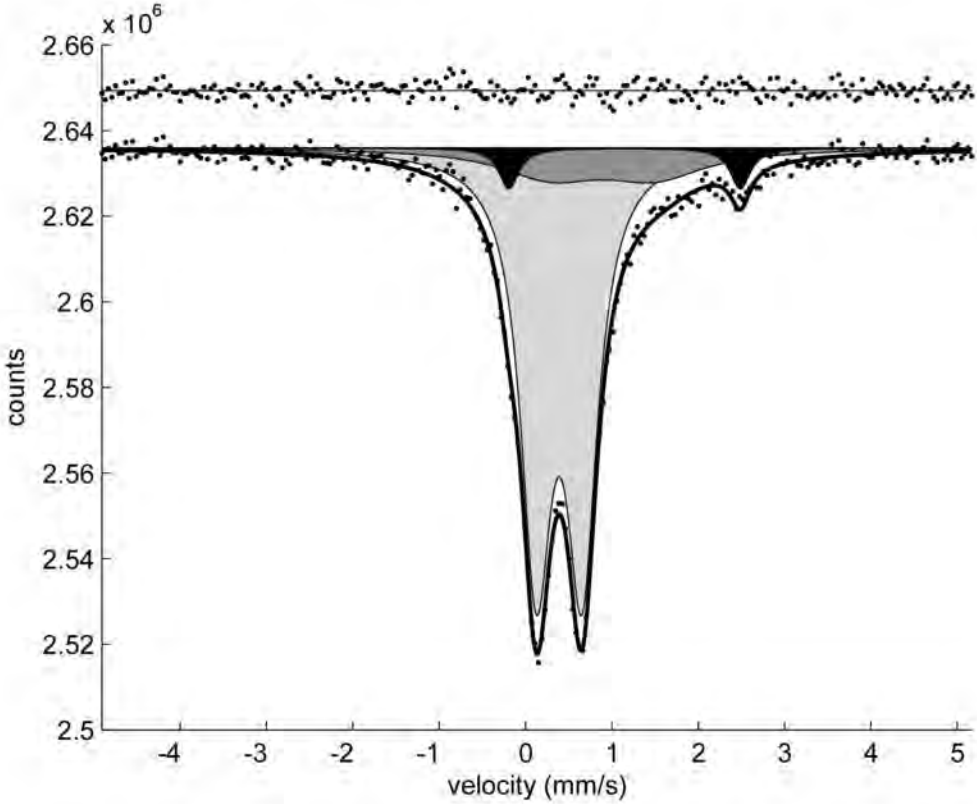
x 10^6
2.66
2.64
2.62
2.6
2.58
2.56
2.54
2.52
2.5
counts
-4
-3
-2
-1
0
1
2
3
4
5
velocity (mm/s)